

Modelling Resistive Wall Mode feedback control in Flexi-DEMO upper operational point

L. Pigatto¹, T. Bolzonella¹, E. Fable², Y. Q. Liu³, M. Siccinio^{2,4}

¹ *Consorzio RFX (CNR, ENEA, INFN, Università di Padova, Acciaierie Venete SpA), Corso Stati Uniti 4 – 35127 – Padova (Italy)*

² *Max-Planck-Institut für Plasmaphysik, Boltzmannstr. 2, D-85748 Garching, Germany*

³ *General Atomics, PO Box 85608, San Diego, CA 92186-5608, USA*

⁴ *EUROfusion Consortium, Boltzmannstr.2, D-85748 Garching, Germany*

Resistive Wall Mode instabilities [1] are ideal MHD modes that develop in Tokamaks usually when the normalized kinetic to magnetic pressure exceeds the so-called no-wall limit. These instabilities are slowed down by the presence of passive structures and grow on the time scale of the magnetic field penetration through the resistive wall. According to the present understanding and developing theories, RWMs can interact with a variety of particle motions (e.g. trapped particle precession and bounce) depending on the interaction between plasma flow and the particle motion characteristic frequencies. Robust experimental evidence of these interactions, along with the possible beneficial effects for RWM stabilization, has been built over the last decade [2][3][4]. Another option to deal with RWMs is that of magnetic feedback, made possible by the mode growing on wall penetration time scales. Again extensive modelling and experimental work has been carried out on the subject, demonstrating that RWM active control is possible in both Tokamak (mostly pressure-driven) and Reversed Field Pinch (current-driven) devices [5][6]. The target of the present work is a linear investigation of RWM stability for the upper operational point of Flexi-DEMO, an intermediate step between ITER and future power plants in the so-called stepladder approach to fusion power [7]. The work has been carried out with the linear stability code MARS-F [8]. This code solves linearized MHD equations in full toroidal geometry (single n , spectral in m) with the possibility of modelling magnetic feedback with a simplified representation of external coils. In MARS-F the coils are modeled as divergence-free surface current perturbations, with delta-like functions of finite poloidal width at the poloidal locations of the coils. The toroidal dependence is $e^{in\phi}$, with n the toroidal mode number. MARS-F has been extensively applied to many present day fusion experiments, and for predictive modeling on

Flexi-DEMO equil.	
l_i	0.6
q_a	6.3
R_0	8.4 m
B_0	5.8 T
R/a	2.9
I_p	14.5 MA
β_N	3

Table 1 – Target plasma main parameters

future devices including ITER [9]. The Flexi-DEMO upper operational point scenario has been simulated with the ASTRA code [10]. A flat-top time instant has been selected for stability analyses. This equilibrium relies on high fraction of auxiliary current drive and shows a safety factor profile optimized for bootstrap maximization. Stability of the most unstable RWM in this plasma studied with a fluid model. Plasma flow is expected to be small in this DEMO scenario and it is neglected in the model. Therefore no RWM damping model is used (either fluid or

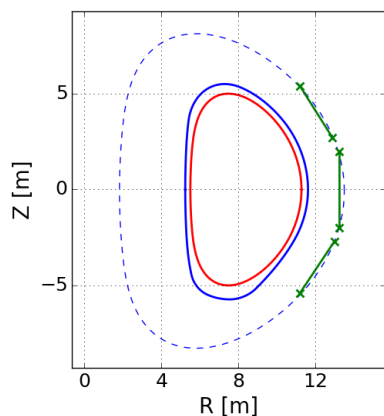


Figure 1 - Coil geometry and 2D boundaries implemented in MARS-F. (Red solid) plasma boundary. (Blue solid) selected position for the resistive wall. (Blue dashed) Surface for coils.

kinetic triggered by plasma flow). The target equilibrium for MARS-F modelling has been solved with the CHEASE equilibrium code (Table 1). Stability limits for the $n=1$ pressure-driven external kink have been calculated with the MARS-F code. The no-wall and ideal-wall stability limits are $\beta_N^{no-w} = 2.0$, $\beta_N^{id-w} = 4.5$. The $n=1$ ideal kink is found to be the first instability to be triggered as pressure increases. For this reason, only the $n=1$ mode will be considered in the present work. The position for the ideal wall (and conducting wall afterwards) has been calculated for the target scenario ($\beta_N \sim 3$) with a scan of plasma-wall distance and set to $r/a = 1.08$. The ELM coils are assumed to be used for RWM stabilization [11]. This choice is based on the assumption that an extra coil system, solely for RWM stabilization, might not be possible to install on a DEMO-like device. Multi-purpose coils, provided the necessary flexibility in power supplies and coil design, could be a good solution for a variety of applications. The RWM growth rate with the aforementioned wall is $\gamma\tau_w \sim 7$, which is a rather fast instability, considering the standard RWM regime being $\gamma\tau_w \sim 1$. For magnetic feedback, current control logic is assumed, with an ideal amplifier. The Plasma Response Model approach has been used to calculate the open-loop transfer function of the system and assess closed-loop stability with the Nyquist criterion.

kinetic triggered by plasma flow). The target equilibrium for MARS-F modelling has been solved with the CHEASE equilibrium code (Table 1). Stability limits for the $n=1$ pressure-driven external kink have been calculated with the MARS-F code. The no-wall and ideal-wall stability limits are $\beta_N^{no-w} = 2.0$, $\beta_N^{id-w} = 4.5$. The $n=1$ ideal kink is found to be the first instability to be triggered as pressure increases. For this reason, only the $n=1$ mode will be considered in the present work. The position for the ideal wall (and conducting wall afterwards) has been calculated for the target scenario ($\beta_N \sim 3$) with a scan of plasma-wall distance and set to $r/a = 1.08$. The ELM coils are assumed to be used for RWM stabilization

[11]. This choice is based on the assumption that an extra coil system, solely for RWM stabilization, might not be possible to install on a DEMO-like device. Multi-purpose coils, provided the necessary flexibility in power supplies and coil design, could be a good solution

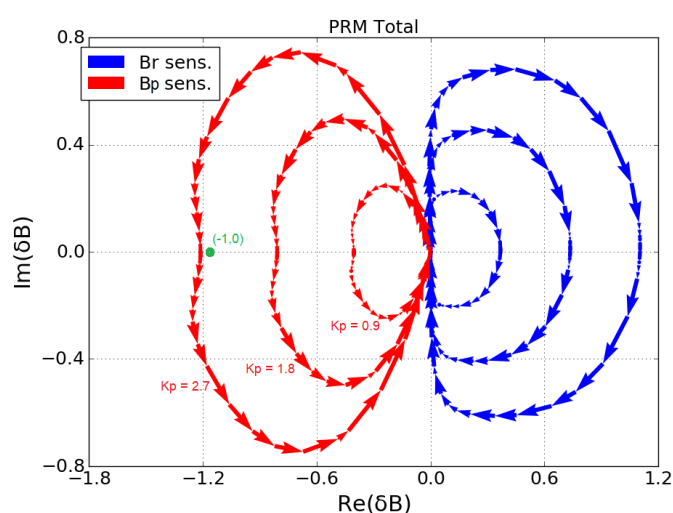


Figure 2 - Nyquist plot of the open-loop transfer function for the 3-coil system with optimal phasing. Both poloidal and radial field sensors are plotted. The transfer function is scaled with the proportional gain $K_P \cdot P_{tot}(j\omega)$

For each single coil, the PRM has been obtained by full toroidal calculations with MARS-F [12]:

$$P(s) = P(j\omega) = \frac{\Psi(j\omega)}{M_{sf}I_f}$$

Where $\Psi(j\omega)$ is the sensor flux, M_{sf} the sensor-coil mutual inductance ($\omega = 0$) used for normalization and I_f the coil current. Closed-loop stability with negative feedback and a general controller $G(s)$ is determined by the characteristic equation:

$$1 + G(s)P(s) = 0$$

$$G = |G|e^{i\pi(\angle G)}$$

The PRM for the complete 3-coil system ($P_{tot}(s)$) is obtained from a linear combination of single coil responses, and the Nyquist criterion can be applied to assess the stability of a single pole closed-loop system from the total PRM (Figure 2)

$$P_{tot}(j\omega) = P_M(j\omega) + e^{j\phi_U}P_U(j\omega) + e^{j\phi_L}P_L(j\omega)$$

A scan of the phasing between upper and lower coils (i.e. the phase of the complex gains) has been carried out to assess the optimal phasing to achieve a stabilizing effect. Stabilization of the closed-loop system, according to the Nyquist criterion, is achieved with $\phi_U = +\frac{\pi}{2}$ and $\phi_L = -\frac{\pi}{2}$. In particular, the system can only be stabilized using poloidal field sensors, with a proportional gain of $K_p \sim 2.6 - 2.7$. The same result is recovered by direct feedback runs of the MARS-F, i.e. solving the eigenvalue problem for the closed-loop system while varying K_p at each step. In Figure 3 the complex gain applied for feedback control has been scanned with the optimal coil phasing discussed above. Direct eigenvalue runs also confirmed that only poloidal field sensors are effective in stabilizing the RWM. A time-stepping simulation has been carried out to evaluate the amplitude of the perturbed field

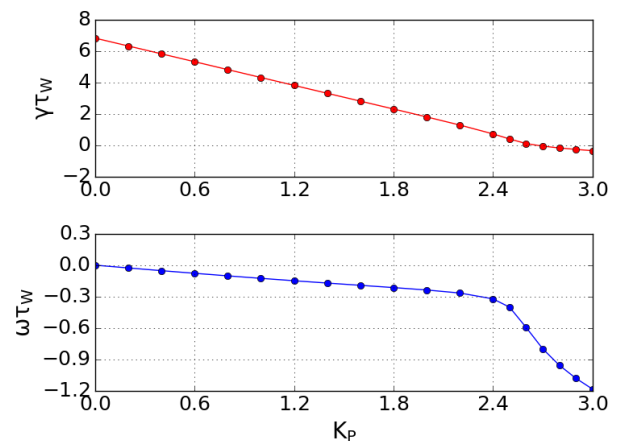


Figure 3 - Growth rate (upper) and rotation frequency (bottom) of the n=1 RWM with varying proportional gain for poloidal field sensors.

at sensor position. The amplitude of the perturbation given by the RWM instability and the control fields can be used to evaluate the impact on particle confinement. A threshold of 250 Gauss has been assumed for switching on feedback control. The feedback logic is the same used for the previous analyses: proportional control with 90° phasing between coils and ideal current amplifier. To check the consistency of the time simulation, the output field has been

extracted for a mid-plane pick-up sensor located at $R=11.52$ m (on the inner side of the resistive wall). The perturbed field at sensor position is ~ 150 Gauss, while inside the plasma the perturbation is ~ 1000 Gauss. Figure 4 shows a contour plot of the perturbed magnetic field

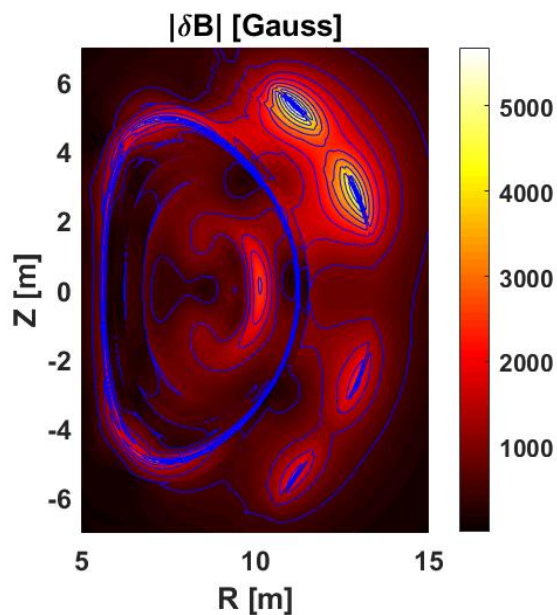


Figure 4 - Absolute value of magnetic field perturbation on R-Z grid

magnitude in plasma and vacuum domains, for a controlled RWM. Conclusions and outlook.

The linear stability of $n=1$ Resistive Wall Modes has been studied for the Flexi-DEMO upper operational point using both the plasma response model approach and direct feedback runs. The two methods yield consistent results in stabilizing the target mode with proportional feedback, current control with poloidal field sensors. Initial value runs have been carried out to simulate RWM control in time, setting a feedback turn-on threshold. Results indicate that the controlled mode still produces a strong

perturbation in the plasma region, which could deeply affect particle confinement. Passive RWM stabilization mechanisms are likely to occur in the investigated plasma scenario and should be taken into account in the study. Including drift-kinetic physics of alpha particles for example, could lead to significant mode damping and play alongside magnetic feedback for realistic RWM stabilization. Finally, reducing the plasma-coil gap by using in-vessel coils would likely be beneficial for RWM feedback, this is feasible in the investigated scenario if the resistive wall can be pushed further away from the plasma by exploiting passive damping channels.

Part of the data analysis was performed using the OMFIT integrated modeling framework [13]. This work has been carried out within the framework of the EUROfusion Consortium and has received funding from the Euratom research and training programme 2014-2018 and 2019-2020 under grant agreement No 633053. The views and opinions expressed herein do not necessarily reflect those of the European Commission.

- [1] Chu M.S. and Okabayashi M. 2010 Plasma Phys. Control. Fusion 52 123001
- [2] Chapman I.T. et al 2009 JET Plasma Phys. Control. Fusion 51 055015
- [3] Berkery J.W. et al 2010 Phys. Plasmas 17 082504
- [4] Takechi M. et al 2007 Phys. Rev. Lett. 98 055002
- [5] Garofalo A.M. et al 2007 Nucl. Fusion 47 1121
- [6] Zanca P. et al 2007 Nucl. Fusion 47 1425T
- [7] Zohm, H. et al 2017 Nucl. Fusion 57 086002
- [8] Liu Y.Q. et al 2000 Phys. Plasmas 7 3681–90
- [9] Liu Y.Q. et al 2005 Nucl. Fusion 45 1131
- [10] Siccino, M. et al In: 2018 IAEA Fusion Energy Conf
- [11] Zhou, L. et al 2018 Nucl. Fusion 58 076025
- [12] Liu, Y.Q. 2017 Computer Physics Communications 176 161–169
- [13] Meneghini, O. et al 2015 Nucl. Fusion 55 083008